Motion Control of Two-Link Flexible-Joint Robot with Actuator Nonlinearities, Using Backstepping and Neural Networks

Withit Chatlatanagulchai and Peter H. Meckl

School of Mechanical Engineering
Purdue University
West Lafayette, Indiana, USA

{chatlata, meckl}@purdue.edu

***Abstract*—We present a state-feedback control of a two-link flexible-joint robot. The control algorithm does not require the mathematical model representing the robot. Three-layer neural networks approximate the unknown plant functions. The neural network weights are adapted on-line. We use backstepping control structure. We use variable structure control to provide robustness to all uncertainties. For simulation, we obtain parameter values of the Euler-Lagrange model from real experiment. We, then, add backlash, deadzone, and additive disturbances to the Euler-Lagrange model to closely replicate the actual robot. We show through simulation that our controller can handle these actuator nonlinearities effectively.**

Index Terms – Flexible-joint robot, Intelligent control, Backstepping, Variable structure control.

I. Introduction

The experiment in [1] suggested that the designers should consider joint flexibility in both modeling and control design. However, controller design of two-link flexible-joint robot is challenging due to two main reasons. First, its Euler-Lagrange model is more complicated than those of rigid-joint or one-link flexible-joint robot. Second, the number of degree of freedom is twice the number of control inputs.

There exist some well-established control designs for flexible-joint robots. In [2], they transform the dynamical model of the flexible-joint robot into the standard singular perturbation model, by using link position as slow variable and joint torque as fast variable. Controller is a composite of slow and fast control. Slow-control input, which adds damping to the system, drives the closed-loop system to a quasi-steady state system that has the structure of a rigid-joint robot. Then, fast-control input can be designed using available techniques for the rigid-joint robot. To avoid having to measure the joint torque signal, you may consult [3] for a design of an observer. Reference [4] shows an alternative singular perturbation model by using tracking error of motor shaft as fast variable. Reference [5] extends the work in [2] to the case where model uncertainties exist in the system. They use radial basis function networks to estimate unknown functions, and use discontinuous variable-structure controller to provide the closed-loop system with robustness for the estimation errors.

Under the assumption that the kinetic energy of the motor is due mainly to its own rotation, the flexible-joint robot model is feedback linearizable by static feedback control laws as in [6]. Reference [7] relaxes this assumption, and applies the so-called dynamic feedback linearization method to a more general robot model.

Reference [8] compares three types of controllers: controller developed from decoupled model, backstepping controller, and passivity-based controller. For the first type, they interestingly decouple the robot model by using filtered error of link position and motor position error as variables. They also discuss backstepping controller when model parameters are unknown but can be made to appear linearly with respect to known functions. Passivity-based controller is designed to shape the closed-loop total energy to desired value to achieve passivity.

Some of the more recent work are [9]-[12]. Reference [9] has experiment result on one-link flexible-joint robot in vertical plane. Reference [10] uses feedback linearization method and Takagi-Sugeno fuzzy system to replace model uncertainties. Reference [11] contains good references on flexible-joint and flexible-link robots. Reference [12] is written from practitioner's point of view.

This paper has following features:

1) Actuator nonlinearities, i.e., deadzone and backlash are added to the Euler-Lagrange model. These actuator nonlinearities always exist in practice, and controller implementation usually requires additional sensors to measure their magnitude. Our control algorithm only requires their magnitude to be bounded; we do not need additional sensors. We also add external additive disturbances, commonly found in practice in the forms of measurement noise and vibration to the Euler-Lagrange model.

2) The controller algorithm does not require closed-form mathematical model of the robot. We use a three-layer neural network to represent each unknown function. Uncertainties come from the estimation of plant functions, actuator nonlinearities, and external disturbance. We use smooth version of variable structure controller to provide robustness to the system, under the assumption that all uncertainties are bounded by unknown bounds. Backstepping structure provides a way to insert control effort to each subsystem.

3) We are able to control the trajectory of the robot

effectively using link angular position, link angular velocity, motor angular position, and motor angular velocity. Existing work usually requires, in addition to the quantities above, link angular acceleration and jerk, or flexible-joint torque.

We organize this paper as follows. Section II contains the Euler-Lagrange model of the robot, and actuator nonlinearities models. Section III contains three-layer neural network background and controller design. Section IV contains simulation result. Section V is conclusion.

II. Robot Model

The controller algorithm presented in this paper does not require explicitly the plant functions. However, to be able to perform stability proof, we assume that the actual plant has the form

$$\begin{aligned} \dot{x}_i &= f_i\left(\bar{x}_m\right) + g_i\left(\bar{x}_m\right) x_{i+1}, 1 \le i \le m-1, \\ \dot{x}_m &= f_m\left(\bar{x}_m\right) + g_m\left(\bar{x}_m\right) T, \\ y &= x_1, \end{aligned} \tag{1}$$

where $T = \left[T_1, \ldots, T_n\right]^T \in \mathbb{R}^n$ represents input to the system, $x_i = \left[x_{i1}, \ldots, x_{in}\right]^T \in \mathbb{R}^n$ represents state subvector, $y = \left[y_1, \ldots, y_n\right]^T \in \mathbb{R}^n$ is system output, $\bar{x}_m$ denotes the set $\left\{x_1, \ldots, x_m\right\}$, and $f_i \in \mathbb{R}^n$, $g_i \in \mathbb{R}^{n \times n}$, are vector and matrix of unknown smooth functions that may depend on all states.

A. Dynamical Model

Consider a schematic diagram of a two-link flexible-joint robot in Fig. 1.

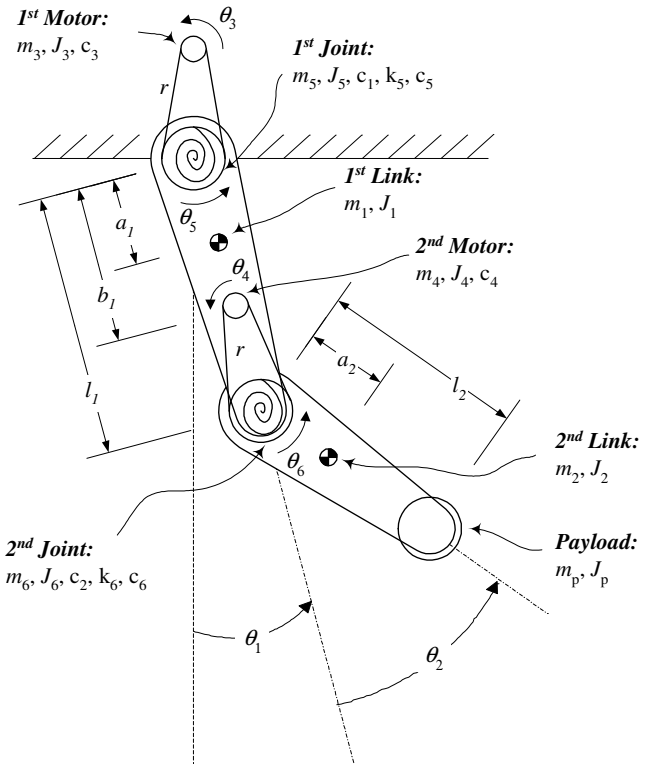

Fig. 1. Schematic diagram of a planar two-link flexible-joint robot.

Let $x_1 = \left[\theta_1, \theta_2\right]^T$ and $x_2 = \left[\dot{\theta}_1, \dot{\theta}_2\right]^T$ represent link position and velocity, $x_3 = \left[\theta_5, \theta_6\right]^T$ and $x_4 = \left[\dot{\theta}_5, \dot{\theta}_6\right]^T$ represent sprocket position and velocity, and $T = \left[T_1, T_2\right]^T$ represent input torque. The Lagrange equations can be put in the following form

$$\begin{aligned} M\dot{x}_2 + Vx_2 + F_1 + B_1\left(x_2 - x_4\right) + K_1\left(x_1 - x_3\right) &= 0, \\ J\dot{x}_4 + F_2 - B_2\left(x_2 - x_4\right) - K_2\left(x_1 - x_3\right) &= T. \end{aligned} \tag{2}$$

The inertia matrix is

$$M\left(x_1\right) = \begin{bmatrix} M_{11} & M_{12} \\ M_{21} & M_{22} \end{bmatrix},$$

$$\begin{aligned} M_{11} &= m_1 a_1^2 + m_2\left(l_1^2 + a_2^2\right) + m_4 b_1^2 + m_6 l_1^2 + J_1 + J_2 \\ &\quad + m_p\left(l_1^2 + l_2^2\right) + J_p + 2l_1\left(m_2 a_2 + m_p l_2\right)\cos\left(\theta_2\right), \\ M_{12} &= M_{21} = m_2 a_2^2 + J_2 + m_p l_2^2 + J_p \\ &\quad + l_1\left(m_2 a_2 + m_p l_2\right)\cos\left(\theta_2\right), \\ M_{22} &= m_2 a_2^2 + J_2 + m_p l_2^2 + J_p. \end{aligned}$$

$V\left(x_1, x_2\right)x_2$ represents coriolis and centrifugal functions and is given by

$$V\left(x_1, x_2\right) = \begin{bmatrix} 0 & -l_1\left(m_2 a_2 + m_p l_2\right) \\ & \left(2\dot{\theta}_1 + \dot{\theta}_2\right)\sin\left(\theta_2\right) \\ l_1\left(m_2 a_2 + m_p l_2\right) & 0 \\ \dot{\theta}_1 \sin\left(\theta_2\right) & \end{bmatrix}.$$

K_1, K_2 are joint flexibility matrices

$$K_1 = \begin{bmatrix} k_5 & 0 \\ 0 & k_6 \end{bmatrix}, K_2 = \begin{bmatrix} k_5 / r & 0 \\ 0 & k_6 / r \end{bmatrix}.$$

J represents the inertia of motors and sprockets

$$J = \begin{bmatrix} r\left(J_3 + J_5 / r^2\right) & 0 \\ 0 & r\left(J_4 + J_6 / r^2\right) \end{bmatrix}.$$

B_1, B_2 contain internal damping of the torsional springs

$$B_1 = \begin{bmatrix} c_5 & 0 \\ 0 & c_6 \end{bmatrix}, B_2 = \begin{bmatrix} c_5 / r & 0 \\ 0 & c_6 / r \end{bmatrix}.$$

$F_1\left(x_2\right), F_2\left(x_4\right)$ are viscous friction vectors

$$F_1\left(x_2\right) = \begin{bmatrix} c_1\dot{\theta}_1 \\ c_2\dot{\theta}_2 \end{bmatrix}, F_2\left(x_4\right) = \begin{bmatrix} rc_3\dot{\theta}_5 \\ rc_4\dot{\theta}_6 \end{bmatrix}.$$

Let $d_{ai}\left(\bar{x}_4\right) = \left[d_{ai1}, d_{ai2}\right]^T$ be additive disturbance that may depend on all states. We, then, obtain the following state-space model

$$\begin{aligned} \dot{x}_1 &= x_2 + d_{a1}\left(\bar{x}_4\right), \\ \dot{x}_2 &= f_2\left(\bar{x}_4\right) + g_2\left(\bar{x}_4\right)\left(x_3 + d_{a2}\left(\bar{x}_4\right)\right), \\ \dot{x}_3 &= x_4 + d_{a3}\left(\bar{x}_4\right), \\ \dot{x}_4 &= f_4\left(\bar{x}_4\right) + g_4\left(\bar{x}_4\right)\left(T + d_{a4}\left(\bar{x}_4\right)\right), \\ y &= x_1, \end{aligned} \tag{3}$$

where

$f_2 = -M^{-1}\left[Vx_2 + F_1 + B_1\left(x_2 - x_4\right) + K_1\left(x_1\right)\right] = \left[f_{21}, f_{22}\right]^T$,

$$g_2 = M^{-1}K_1 = \begin{bmatrix} g_{211} & g_{212} \\ g_{221} & g_{222} \end{bmatrix},$$

$$f_4 = -J^{-1}\left[F_2 - B_2(x_2 - x_4) - K_2(x_1 - x_3)\right] = [f_{41}, f_{42}]^T,$$

$$g_4 = J^{-1} = \begin{bmatrix} g_{411} & g_{412} \\ g_{421} & g_{422} \end{bmatrix}.$$

The model above is in the form (1), which shows its applicability to the controller design in Section III.

To simulate closely the actual robot, we obtain the parameter values of the dynamical model (2) from real experiment. We obtain the plant parameters as follows:

$$M(x_1) = \begin{bmatrix} 0.201 + 0.06\cos\theta_2 & 0.0266 + 0.03\cos\theta_2 \\ 0.0266 + 0.03\cos\theta_2 & 0.0266 \end{bmatrix},$$

$$J = \begin{bmatrix} 0.017 & 0 \\ 0 & 0.014 \end{bmatrix}, \quad (4)$$

$$V(x_1, x_2) = \begin{bmatrix} 0 & -0.03(2\dot{\theta}_1 + \dot{\theta}_2)\sin\theta_2 \\ 0.03\dot{\theta}_1 \sin\theta_2 & 0 \end{bmatrix},$$

$$K_1 = \begin{bmatrix} 0.4 & 0 \\ 0 & 0.4 \end{bmatrix}, K_2 = \begin{bmatrix} 0.075 & 0 \\ 0 & 0.075 \end{bmatrix},$$

$$B_1 = \begin{bmatrix} 0.016 & 0 \\ 0 & 0.016 \end{bmatrix}, B_2 = \begin{bmatrix} 0.003 & 0 \\ 0 & 0.003 \end{bmatrix},$$

$$F_1(x_2) = \begin{bmatrix} 0.02\dot{\theta}_1 \\ 0.02\dot{\theta}_2 \end{bmatrix}, F_2(x_4) = \begin{bmatrix} 0.056\dot{\theta}_5 \\ 0.056\dot{\theta}_6 \end{bmatrix}.$$

We will use this plant to represent actual robot in our simulation in Section IV.

B. Actuator Nonlinearities

Deadzone is a static nonlinearity that describes insensitivity of system to small input signal. Mathematical model of deadzone is given in [13] as follows:

$$\tau = \begin{cases} m^-(u - d^-), & u \le d^-, \\ 0, & d^- < u < d^+, \\ m^+(u - d^+), & u \ge d^+, \end{cases} \quad (5)$$

where τ is output of deadzone model, u is input to the model, m^-, m^+, d^+ are positive numbers, and d^- is a negative number.

Backlash is the difference between tooth space and tooth width of mechanical gearing system. A backlash model as in [14] is given by

$$\dot{T} = \begin{cases} m\dot{\tau}, & \text{if } \dot{\tau} > 0 \text{ and } T = m(\tau - d^+) \text{ or} \\ & \text{if } \dot{\tau} < 0 \text{ and } T = m(\tau - d^-), \\ 0, & \text{otherwise}, \end{cases} \quad (6)$$

where T is output of backlash model, τ is input to the model, m, d^+ are positive numbers and d^- is a negative number.

Fig. 2 depicts the overall plant model where u is the designed control input, τ is output of the deadzone model and T is output of the backlash model which is the input torque actually drive the manipulators. Both τ and T usually cannot be measured directly. Note that, even though deadzone and backlash change the magnitude of the designed control input u, the difference $\|u - T\|$ is bounded.

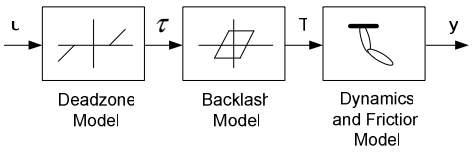

Fig. 2. Deadzone and backlash models are incorporated into the dynamical model of the two-link flexible-joint manipulators.

III. Controller Design

We start this section by discussing basics of the neural network used to estimate the unknown plant function. We, then, discuss how to design a controller based on backstepping structure and how to design a variable structure controller to handle the uncertainties.

A. Three-Layer Neural Network

Each unknown scalar function is replaced by a three-layer neural network. Suppose a scalar-valued continuous function $g(z_1, z_2, \ldots, z_n): \mathbb{R}^n \to \mathbb{R}$ is to be replaced by the neural network. We have $z_1, z_2, \ldots, z_n, 1$ as inputs to the neural network. Variables in the network can be defined as follows:

$$\bar{Z} = [z_1, z_2, \ldots, z_n, 1]^T \in \mathbb{R}^{n+1},$$

$$V = [v_1, v_2, \ldots, v_l] \in \mathbb{R}^{(n+1)\times l},$$

$$v_i = \left[v_{i1}, v_{i2}, \ldots, v_{i(n+1)}\right]^T \in \mathbb{R}^{n+1}, i = 1, 2, \ldots, l,$$

$$S\left(V^T\bar{Z}\right) = \left[s\left(v_1^T\bar{Z}\right), s\left(v_2^T\bar{Z}\right), \ldots, s\left(v_l^T\bar{Z}\right), 1\right]^T \in \mathbb{R}^{l+1},$$

$$W = \left[w_1, w_2, \ldots, w_l, w_{l+1}\right]^T \in \mathbb{R}^{l+1},$$

$$g(W, V, z_1, z_2, \ldots, z_n) = W^T S\left(V^T\bar{Z}\right) \in \mathbb{R},$$

$$s(x) = 1/\left(1 + e^{-x}\right), \forall x \in \mathbb{R}.$$

This network can uniformly approximate any scalar-valued continuous function to any arbitrary accuracy with some constant ideal weights W^*, V^*, and some appropriate number of hidden-layer nodes, l^*, as was proved in [15]. From the universal approximation property, we have

$$g(z_1, z_2, \ldots, z_n) = W^{*T} S(V^{*T}\bar{Z}) + \varepsilon, \quad (7)$$

where $\|\varepsilon\| < \varepsilon_U$ is approximation error with unknown $\varepsilon_U > 0$ providing that $g(\cdot)$ is defined on a compact set Ω_z.

Assumption 1: On the compact set Ω_z, the ideal neural network weights W^*, V^* are constant and bounded by $\|W^*\| \le W_U$, $\|V^*\|_F \le V_U$, $i = 1, \ldots, m$, where W_U and V_U are unknown.

Note that the neural network weight V appears nonlinearly. According to [16], approximators that are nonlinear in their parameters can achieve the same level of approximation accuracy as those that are linear and usually require fewer number of adjusting parameters. However, since the parameter appears nonlinearly, parameter-tuning law is usually more complicated.

Since ideal weights are unknown, let $\hat{W}$ and $\hat{V}$ be the

estimates of W^* and V^* respectively. The estimate of the function g is given by

$$\hat{g}(z_1, z_2, \ldots, z_n) = \hat{W}^T S\left(\hat{V}^T \bar{Z}\right). \tag{8}$$

By using Lemma 3.6 in [17], the difference between neural network output with ideal and estimated weights are given by

$$\begin{aligned} \hat{W}^T S(\hat{V}^T \bar{Z}) - W^{*T} S(V^{*T} \bar{Z}) &= \tilde{W}^T (\hat{S} - \hat{S}' \hat{V}^T \bar{Z}) \\ &\quad + \hat{W}^T \hat{S}' \tilde{V}^T \bar{Z} + d_u, \end{aligned} \tag{9}$$

where $\tilde{W} = \hat{W} - W^*, \tilde{V} = \hat{V} - V^*, \hat{S} = S(\hat{V}^T \bar{Z}) \in \mathbb{R}^{l+1}$,

$$\hat{S}' = diag\left\{\hat{s}_1', \hat{s}_2', \ldots, \hat{s}_l', 0\right\} \in \mathbb{R}^{(l+1)\times(l+1)},$$

$$\hat{s}_i' = s'(\hat{v}_i^T \bar{Z}) = \left.\frac{d[s(z_a)]}{dz_a}\right|_{z_a = \hat{v}_i^T \bar{z}} \in \mathbb{R}, i = 1, 2, \ldots, l,$$

$$s(x) = 1/(1 + e^{-x}), \forall x \in \mathbb{R}.$$

The residual term d_u is bounded by

$$|d_u| \le \left\|V^*\right\|_F \left\|\bar{Z}\hat{W}^T \hat{S}'\right\|_F + \left\|W^*\right\| \left\|\hat{S}' \hat{V}^T \bar{Z}\right\| + \left|W^*\right|_1. \tag{10}$$

B. Backstepping and Variable Structure Controller

In this section, we design a controller that can achieve globally uniformly ultimately bounded tracking error. We require the following assumptions.

Assumption 2: The additive disturbance $d_{aik}(\bar{x}_4)$, where $i = 1, \ldots, 4, k = 1, 2,$ is bounded by $\left\|d_{aik}(\bar{x}_4)\right\| < d_{aikU}$, where d_{aikU} is unknown constant.

Assumption 3: There exists known constant $g_{ijkU} > 0$ such that $\left\|g_{ijk}(\cdot)\right\| \le g_{ijkU}$, $\forall i = 2, \forall j = 1, 2, \forall k = 1, 2.$

Assumption 4: The desired trajectory x_{1d} is smooth.

Assumption 5: There exists unknown constant $T_{iU} > 0$ such that $\left\|T_i - u_i\right\| \le T_{iU}$, $\forall i = 1, 2.$

The control objective is to make output $y = x_1$ follow desired trajectory x_{1d} as closely as possible, while all the signals in the closed-loop system are bounded. For convenience, we drop arguments of some functions where appropriate.

In backstepping design, we try to reduce the error between actual state and desired state of each subsystem – having the tracking error be the error of the first subsystem. Let $e_i = \left[e_{i1}, e_{i2}\right]^T = x_i - x_{id}, i = 1, \ldots, 4$ be those errors.

Step 1:

Let the virtual control law of the first subsystem be

$$x_{2d} = -c_1 e_1 + \dot{x}_{1d} + u_{2dvsc} = \left[x_{21d}, x_{22d}\right]^T,$$

where c_1 is a design parameter, u_{2dvsc} is variable structure control law to be designed. From Assumption 2, we have the following inequality

$$\sum_{k=1}^{2}\left\{\left\|d_{a1k}\right\|\right\} \le \sum_{k=1}^{2}\left\{\left\|d_{a1kU}\right\|\right\}.$$

We let the variable structure control law be in the form $u_{2dvsc} = \left[u_{2dvsc1}, u_{2dvsc2}\right]^T$, where

$$u_{2dvscj} = -\hat{K}_{1j}\left(\frac{2}{\pi}\arctan\left(\frac{e_{1j}}{\mu_{1j}}\right)\right),$$

μ_{1j} is a small positive design parameter, $\hat{K}_{1j}$ approximates $\sum_{k=1}^{2}\left\{\left\|d_{a1kU}\right\|\right\}$.

The time derivative of the error of the first subsystem becomes

$$\begin{aligned} \dot{e}_1 &= \dot{x}_1 - \dot{x}_{1d} = \left(x_2 + d_{a1}\right) - \dot{x}_{1d} = \left(e_2 + x_{2d} + d_{a1}\right) - \dot{x}_{1d} \\ &= e_2 - c_1 e_1 + u_{2dvsc} + d_{a1}. \end{aligned}$$

Step 2:

Let the virtual control law of the second subsystem be

$$x_{3d} = -\hat{g}_2^{-1}[e_1 + c_2 e_2 + \hat{f}_2 - \dot{x}_{2d} - u_{3dvsc}] = \left[x_{31d}, x_{32d}\right]^T.$$

From (7), (10), Assumption 2, and Assumption 3, we have

$$\begin{aligned} &\left|d_{uf_{2j}}\right| + \left|\varepsilon_{f_{2j}}\right| + \sum_{k=1}^{2}\left\{\left|d_{ug_{2jk}} x_{3dk}\right|\right\} \\ &+ \sum_{k=1}^{2}\left\{\left|\varepsilon_{g_{2jk}} x_{3dk}\right|\right\} + \sum_{k=1}^{2}\left\{\left|g_{2jk} d_{a2k}\right|\right\} \end{aligned} \quad \le \quad K_{2j}^{*T} \phi_{2j},$$

where

$$\begin{aligned} K_{2j}^* = \Bigg[&\left\|V_{f_{2j}}^*\right\|_F, \left\|W_{f_{2j}}^*\right\|, \left\|W_{f_{2j}}^*\right\|_1 + \varepsilon_{f_{2jU}} + \sum_{k=1}^{2}\left\{g_{2jkU} d_{a2kU}\right\}, \\ &\sum_{k=1}^{2}\left\{\left\|V_{g_{2jk}}^*\right\|_F\right\}, \sum_{k=1}^{2}\left\{\left\|W_{g_{2jk}}^*\right\|\right\}, \sum_{k=1}^{2}\left\{\left\|W_{g_{2jk}}^*\right\|_1\right\} + \sum_{k=1}^{2}\left\{\varepsilon_{g_{2jkU}}\right\}\Bigg]^T, \end{aligned}$$

$$\begin{aligned} \phi_{2j} = \Bigg[&\left\|\bar{Z}_{f_{2j}} \hat{W}_{f_{2j}}^T \hat{S}_{f_{2j}}'\right\|_F, \left\|\hat{S}_{f_{2j}}' \hat{V}_{f_{2j}}^T \bar{Z}_{f_{2j}}\right\|, 1, \\ &\sum_{k=1}^{2}\left\{\left\|\bar{Z}_{g_{2jk}} \hat{W}_{g_{2jk}}^T \hat{S}_{g_{2jk}}' x_{3dk}\right\|_F\right\}, \sum_{k=1}^{2}\left\{\left\|\hat{S}_{g_{2jk}}' \hat{V}_{g_{2jk}}^T \bar{Z}_{g_{2jk}} x_{3dk}\right\|\right\}, \\ &\sum_{k=1}^{2}\left\{\left\|x_{3dk}\right\|\right\}\Bigg]. \end{aligned}$$

The variable structure control law is given by $u_{3dvsc} = \left[u_{3dvsc1}, u_{3dvsc2}\right]^T \in \mathbb{R}^2$, where

$$u_{3dvscj} = -\hat{K}_{2j}^T \bar{\phi}_{2j},$$

$$\bar{\phi}_{2j} = \begin{bmatrix} \left\|\bar{Z}_{f2j} \hat{W}_{f2j}^T \hat{S}_{f2j}'\right\|_F \dfrac{2}{\pi}\arctan\left(\dfrac{e_{2j}}{\mu_{2j}\left\|\bar{Z}_{f2j} \hat{W}_{f2j}^T \hat{S}_{f2j}'\right\|_F}\right) \\ \hline \left\|\hat{S}_{f2j}' \hat{V}_{f2j}^T \bar{Z}_{f2j}\right\| \dfrac{2}{\pi}\arctan\left(\dfrac{e_{2j}}{\mu_{2j}\left\|\hat{S}_{f2j}' \hat{V}_{f2j}^T \bar{Z}_{f2j}\right\|}\right) \\ \hline \dfrac{2}{\pi}\arctan\left(\dfrac{e_{2j}}{\mu_{2j}}\right) \\ \hline \sum_{k=1}^{2}\left\{\left\|\bar{Z}_{g_{2jk}} \hat{W}_{g_{2jk}}^T \hat{S}_{g_{2jk}}' x_{3dk}\right\|_F\right\} \dfrac{2}{\pi} \\ \bullet \arctan\left(\dfrac{e_{2j}}{\mu_{2j}} \sum_{k=1}^{2}\left\{\left\|\bar{Z}_{g_{2jk}} \hat{W}_{g_{2jk}}^T \hat{S}_{g_{2jk}}' x_{3dk}\right\|_F\right\}\right) \\ \hline \sum_{k=1}^{2}\left\{\left\|\hat{S}_{g_{2jk}}' \hat{V}_{g_{2jk}}^T \bar{Z}_{g_{2jk}} x_{3dk}\right\|\right\} \dfrac{2}{\pi} \\ \bullet \arctan\left(\dfrac{e_{2j}}{\mu_{2j}} \sum_{k=1}^{2}\left\{\left\|\hat{S}_{g_{2jk}}' \hat{V}_{g_{2jk}}^T \bar{Z}_{g_{2jk}} x_{3dk}\right\|\right\}\right) \\ \hline \sum_{k=1}^{2}\left\{\left\|x_{3dk}\right\|\right\} \dfrac{2}{\pi}\arctan\left(\dfrac{e_{2j}}{\mu_{2j}} \sum_{k=1}^{2}\left\{\left\|x_{3dk}\right\|\right\}\right) \end{bmatrix}.$$

μ_{2j} is a small positive design parameter, $\hat{K}_{2j}$ approximates K_{2j}^*. The time derivative of the error of the second subsystem becomes

$$\dot{e}_2 = \dot{x}_2 - \dot{x}_{2d}$$

$$= \begin{bmatrix} \varepsilon_{f21} - \tilde{W}_{f21}^T(\hat{S}_{f21} - \hat{S}_{f21}^{'}\hat{V}_{f21}^T\bar{Z}_{f21}) - \hat{W}_{f21}^T\hat{S}_{f21}^{'}\tilde{V}_{f21}^T\bar{Z}_{f21} \\ -d_{uf21} \\ \hline \varepsilon_{f22} - \tilde{W}_{f22}^T(\hat{S}_{f22} - \hat{S}_{f22}^{'}\hat{V}_{f22}^T\bar{Z}_{f22}) - \hat{W}_{f22}^T\hat{S}_{f22}^{'}\tilde{V}_{f22}^T\bar{Z}_{f22} \\ -d_{uf22} \end{bmatrix}$$

$$+ \left[\begin{array}{l|l} \varepsilon_{g211} - \tilde{W}_{g211}^T(\hat{S}_{g211} & \varepsilon_{g112} - \tilde{W}_{g112}^T(\hat{S}_{g112} \\ -\hat{S}_{g211}^{'}\hat{V}_{g211}^T\bar{Z}_{g211}) & -\hat{S}_{g112}^{'}\hat{V}_{g112}^T\bar{Z}_{g112}) \\ -\hat{W}_{g211}^T\hat{S}_{g211}^{'}\tilde{V}_{g211}^T\bar{Z}_{g211} & -\hat{W}_{g112}^T\hat{S}_{g112}^{'}\tilde{V}_{g112}^T\bar{Z}_{g112} \\ -d_{ug211} & -d_{ug112} \\ \hline \varepsilon_{g121} - \tilde{W}_{g121}^T(\hat{S}_{g121} & \varepsilon_{g122} - \tilde{W}_{g122}^T(\hat{S}_{g122} \\ -\hat{S}_{g121}^{'}\hat{V}_{g121}^T\bar{Z}_{g121}) & -\hat{S}_{g122}^{'}\hat{V}_{g122}^T\bar{Z}_{g122}) \\ -\hat{W}_{g121}^T\hat{S}_{g121}^{'}\tilde{V}_{g121}^T\bar{Z}_{g121} & -\hat{W}_{g122}^T\hat{S}_{g122}^{'}\tilde{V}_{g122}^T\bar{Z}_{g122} \\ -d_{ug121} & -d_{ug122} \end{array}\right] x_{3d}$$

$$- e_1 - c_2 e_2 + u_{3dvsc} + g_2 d_{a2} + g_2(x_3 - x_{3d}).$$

Step 3:

Let the virtual control law of the third subsystem be

$$x_{4d} = -g_{2U}e_2 - c_3 e_3 + \dot{x}_{3d} + u_{4dvsc} = [x_{41d}, x_{42d}]^T,$$

where $g_{2U} = \begin{bmatrix} g_{211U} & g_{212U} \\ g_{221U} & g_{222U} \end{bmatrix}$.

Similar to Step 1, we let the variable structure control be in the form $u_{4dvsc} = [u_{4dvsc1}, u_{4dvsc2}]^T$, where

$$u_{4dvscj} = -\hat{K}_{3j}\left(\frac{2}{\pi}\arctan\left(\frac{e_{3j}}{\mu_{3j}}\right)\right),$$

The time derivative of the error of the third subsystem is given by

$$\dot{e}_3 = -g_{2U}e_2 - c_3 e_3 + e_4 + u_{4dvsc} + d_{a3}.$$

Step 4:

Let the desired control law be

$$u = -\hat{g}_4^{-1}[e_3 + c_4 e_4 + \hat{f}_4 - \dot{x}_{4d} - u_{5dvsc}] = [u_1, u_2]^T.$$

The time derivative of the error of the last subsystem, $\dot{e}_4$, can be derived similar to Step 2.

Since the desired control input u differs from the input torque T that actually drives the plant, there is an extra term, $g_4(T-u)$, in the $\dot{e}_4$ equation. However, the difference is bounded according to Assumption 5, and will be treated as an uncertainty, which will appear as an extra term $\sum_{k=1}^{2}\{g_{4jkU}T_{kU}\}$ in K_{4j}^*.

Since K_{4j}^* does not appear in the control law, the variable structure control law, u_{5dvsc}, remains similar to those in Step 2 by replacing x_{3dk} with u_k.

We use the following σ-modification weight updating laws:

$$\dot{\hat{W}}_{fij} = \Gamma_{wfij}[(\hat{S}_{fij} - \hat{S}_{fij}^{'}\hat{V}_{fij}^T\bar{Z}_{fij})z_{ij} - \sigma_{wfij}\hat{W}_{fij}],$$

$$\dot{\hat{V}}_{fij} = \Gamma_{vfij}[\bar{Z}_{fij}\hat{W}_{fij}^T\hat{S}_{fij}^{'}z_{ij} - \sigma_{vfij}\hat{V}_{fij}],$$

$$\dot{\hat{W}}_{gijk} = \Gamma_{wgijk}[(\hat{S}_{gijk} - \hat{S}_{gijk}^{'}\hat{V}_{gijk}^T\bar{Z}_{gijk})x_{(i+1)dk}z_{ij} - \sigma_{wgijk}\hat{W}_{gijk}],$$

$$\dot{\hat{V}}_{gijk} = \Gamma_{vgijk}[\bar{Z}_{gijk}\hat{W}_{gijk}^T\hat{S}_{gijk}^{'}x_{(i+1)dk}z_{ij} - \sigma_{vgijk}\hat{V}_{gijk}],$$

$$\dot{\hat{K}}_{ij} = \Gamma_{kij}[\bar{\phi}_{ij}z_{ij} - \sigma_{kij}\hat{K}_{ij}],$$

where $\Gamma_{wfij}, \Gamma_{vfij}, \Gamma_{wgijk}, \Gamma_{vgijk}, \Gamma_{kij} > 0$; $i = 2,4$; $j = 1,2$; $k = 1,2$. The $\sigma > 0$ terms in the update laws are used to prevent $\hat{W}, \hat{V}, \hat{K}$ from growing unboundedly by maintaining their values around their initial values.

Definition 1: We define $(\bullet^*) = (\hat{\bullet}) - (\tilde{\bullet})$ where $(\bullet^*)$ is the actual or ideal value, $(\tilde{\bullet})$ is estimated error, and $(\hat{\bullet})$ is the estimated value.

Using a Lyapunov function

$$V = \sum_{i=1}^{4}\left\{\frac{1}{2}e_i^T e_i + \sum_{j=1}^{2}\sum_{k=1}^{2}\left[\frac{1}{2}\tilde{W}_{gijk}^T\Gamma_{wgijk}^{-1}\tilde{W}_{gijk} + \frac{1}{2}tr\left(\tilde{V}_{gijk}^T\Gamma_{vgijk}^{-1}\tilde{V}_{gijk}\right)\right] + \sum_{j=1}^{2}\left[\frac{1}{2}\tilde{W}_{fij}^T\Gamma_{wfij}^{-1}\tilde{W}_{fij} + \frac{1}{2}tr\left(\tilde{V}_{fij}^T\Gamma_{vfij}^{-1}\tilde{V}_{fij}\right) + \frac{1}{2}\tilde{K}_{ij}^T\Gamma_{kij}^{-1}\tilde{K}_{ij}\right]\right\},$$

and the following facts

$$2\tilde{W}^T\hat{W} = \left\|\tilde{W}\right\|^2 + \left\|\hat{W}\right\|^2 - \left\|W^*\right\|^2 \geq \left\|\tilde{W}\right\|^2 - \left\|W^*\right\|^2,$$

$$2tr\left\{\tilde{V}^T\hat{V}\right\} = \left\|\tilde{V}\right\|_F^2 + \left\|\hat{V}\right\|_F^2 - \left\|V^*\right\|_F^2 \geq \left\|\tilde{V}\right\|_F^2 - \left\|V^*\right\|_F^2,$$

$$0 \leq |\alpha| - \alpha\frac{2}{\pi}\arctan\left(\frac{\alpha}{\mu}\right) \leq 0.2785\mu, \forall\alpha \in \mathbb{R},$$

and after some straightforward but lengthy derivation, we obtain the derivative of the Lyapunov function as

$$\dot{V} \leq -\varsigma V + \delta,$$

where $\varsigma > 0$ and $\delta \geq 0$.

From this point on, it can be shown using standard nonlinear analysis that the error trajectories $e, \tilde{K}, \tilde{W}, \tilde{V}$ are globally uniformly ultimately bounded.

IV. Simulation

We use the robot model (3) with parameter values from actual experiment (4) to represent the actual robot in our simulation.

We simulate deadzone and backlash by using the following parameters. For deadzone model (5), we have $d^- = -0.1, d^+ = 0.1, m^- = m^+ = 1$. For backlash model (6), we use $d^- = -0.1, d^+ = 0.1, m = 1$. External disturbances are as follows: $d_{a1} = d_{a4} = [0.01\sin(\theta_1\dot{\theta}_1), \arctan(\theta_1\dot{\theta}_2)]^T$, $d_{a2} = d_{a3} = [0.001\,\text{randn}(2,1)]^T$, where *randn* represents white noise.

To simulate payload changes, we multiply $M(x_1)$ and $V(x_1, x_2)$ matrices by three during 15 to 30 s and 45 to 60 s.

All design parameters are as follows:

$l = 3, \Gamma_{wf} = \Gamma_{vf} = \Gamma_{wg} = \Gamma_{vg} = 10,\ \Gamma_k = 1, c_i = 5,$

$\sigma_{wf} = \sigma_{vf} = \sigma_{wg} = \sigma_{vg} = \sigma_k = 0.1, \mu = 1.$

Input saturation limits are set at ± 15. All initial values are set to 0.1. Sampling period is 1 ms. The desired trajectory is obtained from passing square wave signal of amplitude 10,

with zero mean, and 20-second period into the filter $1/(s+2)^3$.

Simulation results are given in Fig. 3. The control system achieves good overall tracking performance as can be seen from the results in part (a) to (d). Both link angular positions θ_1 and θ_2 are able to follow their desired trajectories quite closely. Part (e) and (f) show control inputs that actually drive the plant. Part (g) and (h) show the actual functions f_{21} and f_{22} versus their estimated values $\hat{f}_{21}$ and $\hat{f}_{22}$.

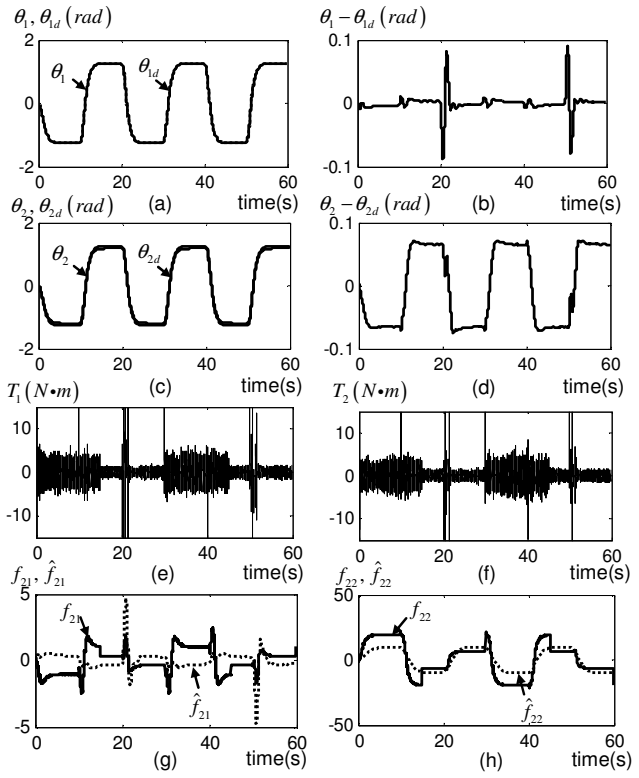

Fig. 3. Simulation result in 60 seconds. (a) θ_1 versus its desired trajectory θ_{1d}. (b) Tracking error $\theta_1 - \theta_{1d}$. (c) θ_2 versus its desired trajectory θ_{2d}. (d) Tracking error $\theta_2 - \theta_{2d}$. (e) Control input T_1. (f) Control input T_2. (g) Actual plant function f_{21} versus estimated function $\hat{f}_{21}$; (h) Actual plant function f_{22} versus estimated function $\hat{f}_{22}$.

V. Conclusion

The controller achieves good tracking performance despite having actuator nonlinearities. The actuator nonlinearities are treated as bounded uncertainties and are handled by variable structure controller. The result of incorporating an observer into this controller is given in [18].

References

[1] L. M. Sweet and M. C. Good, "Re-definition of the robot motion control problem: effects of plant dynamics drive system constraints, and user requirements," *Proc. of 23rd IEEE Conf. on Decision and Control*, Las Vegas, NV, 1984, pp. 724-731.

[2] M. W. Spong, "Modeling and control of elastic joint robots," *Trans. ASME J. Dynamic Systems, Measurement and Control,* vol. 109, no. 4, pp. 310-319, 1987.

[3] S. Nicosia, P. Tomei, and A. Tornambe, "A nonlinear observer for elastic robots," *IEEE J. Robot. Automat.,* vol. 4, no. 1, pp. 45-52, 1988.

[4] S. S. Ge, "Adaptive control design for flexible joint manipulators," *Automatica,* vol. 32, no. 2, pp. 273-278, 1996.

[5] S. S. Ge, T. H. Lee, and C. J. Harris, *Adaptive Neural Network Control of Robotic Manipulators.* Singapore: World Scientific Publishing, 1998, ch. 7.

[6] M. Spong and M. Vidyasagar, *Robot Dynamics and Control.* New York: Wiley, 1989.

[7] A, De Luca and P. Lucibello, "A general algorithm for dynamic feedback linearization of robots with elastic joints," *Proc. of 1998 IEEE Int. Conf. on Robotics and Automation*, Belgium, pp. 504-510.

[8] B. Brogliato, R. Ortega, and R. Lozano, "Global tracking controllers for flexible-joint manipulators: a comparative study," *Automatica,* vol. 31, no. 7, pp. 941-956, 1995.

[9] A. C. Huang and Y. C. Chen, "Adaptive sliding control for single-link flexible-joint robot with mismatched uncertainties," *IEEE Trans. Contr. Syst. Technol.,* vol. 12, no. 5, pp. 770-775, 2004.

[10] C. W. Park, "Robust stable fuzzy control via fuzzy modeling and feedback linearization with its applications to controlling uncertain single-link flexible joint manipulators," *Journal of Intelligent and Robotic Systems,* vol. 39, pp. 131-147, 2004.

[11] B. Subudhi and A. S. Morris, "Singular perturbation approach to trajectory tracking of flexible robot with joint elasticity," *Int. Journal of Systems Science,* vol. 34, no. 3, pp. 167-179, 2003.

[12] A. A. Schaffer and G. Hirzinger, "A globally stable state feedback controller for flexible joint robots," *Advanced Robotics,* vol. 15, no. 8, pp. 799-814, 2001.

[13] G. Tao and P. V. Kokotovic, *Adaptive Control of Systems with Actuator and Sensor Nonlinearities*. New York: Wiley, 1996.

[14] F. L. Lewis, J. Campos, and R. Selmic, *Neuro-Fuzzy Control of Industrial Systems with Actuator Nonlinearities*. Philadelphia: SIAM, 2002.

[15] K. I. Funahashi, "On the approximate realization of continuous mappings by neural networks," *Neural Networks,* vol. 2, pp. 183-192, 1989.

[16] A. R. Barron, "Universal approximation bounds for superpositions of a sigmoid function," *IEEE Trans. Inform. Theory,* vol. 39, no. 3, pp. 930-945, 1993.

[17] S. S. Ge, C. C. Hang, T. H. Lee, and T. Zhang, *Stable Adaptive Neural Network Control*. The Netherlands: Kluwer, 2002.

[18] W. Chatlatanagulchai, H. C. Nho and P. H. Meckl, "Robust observer backstepping neural networks control of flexible-joint manipulator," in *Proc. American Control Conference,* Boston, 2004, pp. 5250-5255.